2018 년 2 월

석사학위 논문

Functional studies on the role of E6AP in hepatic stellate cell activation

조선대학교 대학원

약 학 과

김 지 영

Functional studies on the role of E6AP in hepatic stellate cell activation

간섬유화 신규 표적으로써 E6AP 기능 조절 연구

2018 년 2 월 23 일

조선대학교 대학원

약 학 과

김 지 영

Functional studies on the role of E6AP in hepatic stellate cell activation

지도교수 기 성 환

이 논문을 약학 석사학위신청 논문으로 제출함

2017 년 10 월

조선대학교 대학원

약 학 과

김 지 영

김지영의 석사학위논문을 인준함

위원장 조선대학교 교수 최 홍 석 인

위 원 조선대학교 교수 신 상 미 인

위 원 조선대학교 교수 기 성 환 인

2017 년 11 월

조선대학교 대학원

CONTENTS

LIST OF FIGURES

ABBREVIATIONS

ECM	Extracellular matrix
HSCs	Hepatic stellate cells
E6AP	E6 associate protein
α-SMA	alpha-Smooth muscle actin
PAI-1	Plasminogen activator inhibitor-1
CCl_4	Carbon tetrachloride
TGF-β	Transforming growth factor-beta
Act.D	Actinomycin-D
CHX	Cycloheximide
MG132	Z-Leu-Leu-Leu-al
CQ	Chloroquine
SBE	Smad binding element
MAPK	Mitogen-activated protein kinase
JNK	c-Jun N-terminal kinase
ERK	Extracellular signal-regulated kinases
AP-1	Activator protein 1
HECT	Homologous to the E6AP carboxyl terminus
miR	microRNA
3'-UTR	3'-untranslated region
qRT-PCR	Quantitative reverse transcription-polymerase chain reaction

국 문 초 록

간섬유화 신규 표적으로써 E6AP 기능 조절 연구

김 지 영

지 도 교 수: 기 성 환

약학과

조선대학교 대학원

간은 체 내 다양한 기능을 담당하는 주요 기관으로, 기능이 저하되면 여러 임상적 문제가 발생한다. 과도한 알코올 섭취, 간염바이러스 및 유전 질환 등 다양한 원인에 의한 간세포의 손상은 염증 반응을 유도하며, 이의 만성적 진행은 휴지상태(quiescent state)로 존재하는 간성상세포를 활성화(activated state)하여 콜라겐과 같은 세포외 기질 (ECM)을 과도하게 축적함으로 간섬유화, 간경변증을 유발하며 이는 간 기능 부전에 이르게 한다. 이러한 간섬유화 발병 및 진행 과정 중 간성상세포의 활성화는 중요한 단계로 알려져 있다. 최근 간섬유화 발병 과정에서 ubiquitination-proteasome의 역할에 대한 연구가 진행되고 있다. E3 ubiquitin ligase는 불필요한 단백질에 유비퀴틴이라는 작은 단백질을 결합시킴으로써 특이적으로 단백질 분해를 촉진하는 유비퀴틴화 효소로, 세포의 스트레스 반응 뿐만 아니

라 세포 성장 조절에 대해서도 연구되어 왔으며 간성상세포 활성화 과정을 조절한다고 알려져 있다. 본 연구에서는 '간성상세포 활성화 과정에서 E3 ubiquitin ligase 중 E6AP (E6-associated protein)의 발현 변화 및 역할' 에 관해 탐구하였다. 현재까지, E6AP가 TGF-β (transforming growth factor-β) 신호 전달과 간 섬유화에 미치는 영향에 대해서는 전혀 연구된 바 없다. 먼저, E6AP의 발현 정도를 비교해 보았을 때, 실질세포인 간세포에 비해 간성상세포에서 더 많이 발현되어 있음을 관찰하였다. 간섬유화를 유도하는 CCl_4를 투여한 mouse로부터 분리한 간성상세포 또는 TGF-β를 처리한 LX-2 세포에서 E6AP의 발현이 상향 조절되어 있음을 확인하였다. TGF-β에 의한 E6AP의 상향 조절이 전사적 활성화 또는 단백질 안정화에 의해 조절되지 않으며, 이를 통해 E6AP의 발현이 다른 전사이후 단계 메커니즘에 의해 조절될 것이라 추정하였다. 이를 검증하기 위하여 본 연구자는 TargetScan 7.1 알고리즘을 이용하여 E6AP를 타겟팅하는 마이크로RNA 후보들을 도출하였다. 후보 마이크로RNA 중 miR-302c의 발현이 TGF-β가 처리된 LX-2 세포 또는 활성화된 간성상세포에서 특이적으로 감소하였다. 또한, 실제로 miR-302c가 E6AP의 합성을 저해함을 miR-302c 저해제와 유사체를 사용하여 각각 증명하였다. 이와 더불어, E6AP 과발현은 LX-2 세포에서 TGF-β에 의해 유도된 PAI-1의 발현을 억제하였다. 그러나 이러한 반응은 Smad 신호 전달 경로에 비의존적이었으며, E6AP가 TGF-β 매개 mitogen-activated protein kinase (MAPKs) 인산화 및 AP-1 활성화를 억제하여 섬유화 유전자 발현을 조절함을 관찰하였다. 이와 더불어 E6AP에 의한 AP-1 저해효과는 c-Jun과 c-Fos가 매개됨을 확인하였다. 결론적으로, 본 연구에서는 간성상세포에서 miR-302c의 감소

에 의한 E6AP 상향 조절이 TGF-β에 의해 유도된 MAPK/AP-1 신호 전달 경로의 억제를 통해 간성상세포의 활성화를 억제함을 새롭게 규명하였다. 본 연구 결과는 간성상세포를 조절하는 신규 분자인 E6AP 및 이와 연관된 조절 분자들이 간섬유화 예방 및 치료 표적으로 활용될 수 있음을 제시한다.

I. INTRODUCTION

Liver fibrosis derived from a variety of etiologies, such as hepatitis B or C virus infection, chronic alcohol abuse, non-alcoholic steatohepatitis, cholestasis, and autoimmune hepatitis can advance to fibrosis and cirrhosis, which is a major cause of morbidity and mortality worldwide [1]. Upon repeated injury, the liver undergoes the wound-healing response leading to accumulation of excessive deposition of extracellular matrix (ECM) and impaired organ function [2].

During this process, hepatic stellate cells (HSCs) transdifferentiate from quiescent cells with vitamin A to highly proliferative myofibroblastic cells, and the activated cells are crucial sources for fiber accumulation and contribute to liver fibrosis [3]. Thus, inactivation or elimination of activated HSCs has become a primary target for anti-fibrotic therapy [4]. Unfortunately, to date, there is no established way to modulate HSC activation. Hence, it is necessary to reveal the new regulatory targets and underlying basis of this process to treat liver fibrosis.

The ubiquitin-proteasome pathway has emerged as a critical post-translational modification mechanism that regulates cell proliferation and differentiation, signal transduction, and apoptosis [5]. Protein degradation via ubiquitin proteasome system is delicately controlled within the cell to maintain protein homeostasis and eliminate misfolded or damaged proteins, and involves a cascade of enzymes called E1 (ubiquitin-activating enzyme), E2 (ubiquitin-conjugating enzyme) and E3 (ubiquitin-ligase) [6]. The effects from ubiquitination-triggered degradation are mainly achieved by E3 ubiquitin ligases (E3 ligase), which are crucial for functioning selective recognition of target proteins and subsequent protein degradation. Additionally, several E3 ligases (e.g. Smad ubiquitin regulatory factor 2 (Smurf 2) [7], S-phase

kinase-associated protein 2 (SKP-2), and synoviolin [8]) play an important role in liver fibrosis. Because the ubiquitin-proteasomal degradation pathway tightly regulates TGF-β signaling [9-12], the mainly involved in HSC activation and the ECM accumulation, E3 ligase may have profound effect on the progression of liver fibrosis.

E6-associated protein (E6AP), a member of the HECT (homologous with E6AP C-terminus) family protein, is known as an E3 ligase involved in the degradation of the p53 and various other cell-cycle regulatory proteins [13]. E6AP is encoded by the *Ube3A* locus, which is mutated in a neurological disorder called Angelman Syndrome [14]. A number of studies have demonstrated that E6AP affect the cancer cell malignancy via controlling cell proliferation, senescence and cellular response to oxidative stress [15-17]. Although E6AP has revealed that exacerbates liver cancer by promoting hepatocellular proliferation [18], little information is available on the role of E6AP in liver pathophysiology. Especially, the involvement of E6AP and its regulatory mechanism in the regulation of transforming growth factor-β (TGF-β) signaling and fibrogenesis in HSCs has not been identified.

In this study, we demonstrate that whether TGF-β signaling upregulates E6AP expression in HSCs, if so, what the impact is on HSC activation and how it is regulated. Here, we found E6AP was abundantly expressed in HSCs compared to hepatocytes and was induced in activated HSCs due to dysregulation of a specific microRNA (miR), which suppressed liver fibrogenesis. Ectopic expression of E6AP inhibited TGF-β-mediated activation of mitogen-activated protein kinases (MAPKs), but not Smad phosphorylation. In addition, we showed that c-Jun or c-Fos-dependent AP-1 activity was related to the anti-fibrogenic effect of E6AP. Our findings provide the novel role of the E6AP in HSC activation and extend the basic scientific information on the liver fibrosis.

II. MATERIALS AND METHODS

1. Materials

Antibodies against E6AP was obtained from Santa Cruz Biotechnology (Santa Cruz, CA, USA). Plasminogen activator inhibitor 1 (PAI-1) antibody was purchased from BD Bioscience (Becton, Dickinson and Company, Mountain View, California). Phospho-JNK1/2, JNK1/2, phospho-ERK, ERK, phospho-p38, p38, phospho-SMAD3, phospho-c-Jun, c-Jun, phospho-c-Fos, and c-Fos antibodies were supplied from Cell Signaling Technology (Danvers, Massacchusetts). Horseradish peroxidase-conjugated goat anti-rabbit and anti-mouse antibodies were purchased from Invitrogen (Carlsbad, California). α–SMA, and β-actin antibodies, Z-Leu-Leu-Leu-al (MG132), chloroquine (CQ), and actinomycin-D (ActD) were purchased from Sigma (St. Louis, MO). TGF-β was purchased from R&D Systems (Minneapolis, Minnesota).

2. Cell culture

LX-2 cells (immortalized human activated HSCs) were generously provided by Dr. S.L. Friedmann (Mount Sinai School of Medicine, New York). Cells were plated in 60 mm plates at 1×10^5 cells per well, and cells were grown to 70-80% confluence. Cells were maintained in Dulbecco's Modified Eagle's Medium (DMEM) containing 10% fetal bovine serum (FBS; Hyclone, Logan, Utah), 50 units/ml penicillin/streptomycin at 37℃ in a humidified 5% CO_2 atmosphere. Cells were then washed twice with ice-cold phosphate buffered saline (PBS) before sample preparation.

3. Isolation of Hepatocytes and HSCs

Hepatocytes and HSCs were isolated from the liver of 8-week-old mice (Oriental Bio, Sungnam, Korea). After intubation in the portal vein, the livers were perfused *in situ* with Ca^{2+}-free Hank's balanced saline solution (HBSS) at 37℃ for 15 min and then perfused with the solution containing 0.05% collagenase and Ca^{2+} for 15 min at a flow mice of 10 mL/min. Perfused livers were minced, filtered through 70 uM cell strainer (BD Bioscience), and centrifuged at 50 g for 3 min to separate hepatocytes. Hepatocytes were resuspended in DMEM supplemented with 10% FBS, 100 U/ml penicillin and 100 μg/mL streptomycin, 5 mM HEPEs, and 10 nM dexamethasone. HSCs were isolated according to the previously published method [19]. Briefly, the supernatant was further centrifuged at 500 g for 10 min, resuspended in Ficoll plus Percoll (1:10, GE Healthcare), and centrifuged at 1400 g for 17 min. HSCs were collected from the interface. Quiescent HSCs were cultured for 0 day, and activated HSCs were cultivated for 7 days.

4. Immunoblot analysis

Protein extraction, SDS polyacrylamide gel electrophoresis, and immunoblot analysis were performed as previously reported (Yang et al., 2015). Briefly, the cell lysates were separated by electrophoresis in 7.5% and 12% gels and electrophoretically transferred to a nitrocellulose membrane. The nitrocellulose membrane was incubated with the indicated primary antibody and then incubated with a horseradish peroxidase-conjugated secondary antibody (Invitrogen). Immunoreactive protein was visualized by enhanced chemiluminescence detection kit (Amersham Biosciences, Buckinghamshire, UK). Equal protein loading was verified using β-actin.

5. RNA isolation, semicomparative RT-PCR, and Quantitative RT-PCR analysis

Total RNA was extracted using TRIzol (Invitrogen) according to the manufacturer's instructions. The RNA (2 μg each) was reverse-transcribed using an oligo-d$(T)_{16}$ primers to obtained cDNA. The cDNA obtained was amplified using a high-capacity cDNA synthesis kit (Bioneer, Daejeon, Korea) with a thermal cycler (Bio-Rad, Hercules, California). Amplified products were separated by using 2% agarose gel, stained with ethidium bromide, and visualized by gel documentation system. Quantitative PCR was performed with StepOne system (Applied Biosystems, Foster City, California) using SYBR green premix (Applied Biosystems). The relative levels of the PCR products were determined based on the threshold cycle value. A melting curve analysis was done after amplification to verify the accuracy of the amplicon. Primer sequences were as follows: human E6AP sense 5'-AGGCCATCACGTATGCCAAA-3', and antisense 5'-AGGGAGGCACAGACATAGGT-3'; mouse E6AP sense 5'-ACTGGGGAAAGTGCATCTGG-3', and antisense 5'-TGCTGCAACACTGATCGAGT-3'; human GAPDH sense 5'-GAAGGTGAAGGTCGGAGTC-3', and antisense 5'-GAAGATGGTGATGGGATTTC-3'; mouse GAPDH sense 5'-TGCCCCCATGTTTGTGATG-3', and antisense 5'-TGTGGTCATGAGCCCTTCC-3'. mRNA expression data were normalized to GAPDH. qRT-PCR for miRNA was done using miScript SYBR Green PCR kit (Qiagen, Hiden, Germany) according to the manufacturer's instruction. All results were normalized to U6 small RNA levels measured using the Hs_RNU6B_2 miScript Primer Assay kit (Qiagen). Primer sequences were as follows : miR-302a-3p, 5'-TAAGTGCTTCCATGTTTTGGTGA-3'; miR-302b-3p, 5'-TAAGTGCTTCCATGTTTTAGTAG-3'; miR-302c-3p, 5'-TAAGTGCTTCCATGTTTCAGTGG-3'; miR-302d-3p, 5'-

TAAGTGCTTCCATGTTTGAGTGT-3'. The relative expression values were normalized to the internal control using $2^{-\triangle\triangle Ct}$.

6. Transient transfection and siRNA knockdown experiment

LX-2 cells were transfected with pCMV4 (MOCK) or pCMV4-E6AP (E6AP) for 24 h using Lipofectamine™ 2000 (Invitrogen, San Diego, CA) according to the manufacturer's instructions. For gene silencing, cells were transfected with non-targeting control siRNA (100 pmol) or siRNA directed against E6AP (100 pmol)(Ambion, Austin, TX) for 24 h using Lipofectamine™ 2000. The cells were transfected with a plasmid using Lipofectamine™ 2000 in Eagle's minimum essential medium (MEM) for 3 h. The medium was then changed to MEM containing 1% FBS, and the cells were further incubated for 24 h with or without TGF-β treatment for 3 h.

7. Luciferase assay

Cells were plated in 12-well plates overnight, serum starved for 4 h, and transiently transfected with SBE luciferase plasmid and pRL-TK plasmid (a plasmid that encodes Renilla luciferase and is used to normalize transfection efficacy) in the presence of Lipofectamine™ 2000 (Invitrogen) for 3 h. Transfected cells were allowed to recover in minimum essential media with 1% FBS overnight and then exposed to TGF-β for 3 h. To measure the luciferase activities of AP-1, mock- or E6AP-transfeced cells were replated in 12-well plates overnight, serum-starved for 4 h, and transiently transfected with AP-1 luciferase plasmid and pRL-TK plasmid (a plasmid that encodes *Renilla* luciferase and used to normalize transfection efficacy) in the presence of Lipofectamine™ 2000 reagent for 3 h. Transfected cells were allowed to recover in

minimum essential media with 1% FBS overnight and then exposed to TGF-β for 3 h. The firefly and Renilla luciferase activities of cell lysates were measured using the dual luciferase assay system (Promega, Madison, Wisconsin) according to the manufacturer's instructions. Relative luciferase activities were calculated by normalizing firefly luciferase activities versus that of Renilla luciferase.

8. Plasmid, microRNA mimic or inhibitor transfection

The cells were transfected with a plasmid using Lipofectamine™ 2000 (Invitrogen) in Eagle's minimum essential medium (MEM) for 3 h. The medium was then changed to MEM containing 1% FBS, and the cells were further incubated for 24 h with or without TGF-β treatment. Cells were transiently transfected with 100 nM each of control mimic, miR-302c mimic, miR-302c inhibitor, or respective negative control miRNA using Lipofectamine™ 2000 reagent according to the manufacturer's protocol: miRNA mimic control, has-miR-302c mimic, inhibitor control, and inhibitor has-miR-302c were obtained from Bioneer (Daejeon, Korea).

9. E6AP 3'-UTR luciferase assay

The plasmid containing the Luc-E6AP-3'-untranslated region (UTR) construct (Product ID: HmiT018388-MT06) used in reporter assays was purchased from GeneCopoeia (Rockville, MD, USA). The plasmid contains firefly luciferase fused to the 3'-UTR of human E6AP and E6AP Renilla luciferase that functions as a tracking gene. Luciferase activity assays were performed according to manufacturer protocol. Briefly, LX-2 cells were seeded in 12-well plates, and co-transfected with miR-302c mimic or miR-302 inhibitor and E6AP-3'-UTR reporter. Cells were harvested following transfection for 12 h or 24 h, respectively. Firefly and

Renilla luciferase activities were measured sequentially with the dual luciferase assay kit (GeneCopoeia). The activities were normalized with Renilla luciferase activities and expressed in relative luciferase activity units.

10. Statistical analysis

One-way ANOVA was used to determine significant differences between treatment groups. The Newman–Keuls test was used to determine the significance of the differences between the means of multiple groups. Results are expressed as means ± standard error (S.E.).

III. RESULTS

1. E6AP was up-regulated in activated HSCs

First, we observed E6AP expression in different types of hepatic cells. We found that E6AP showed the highest specifically in HSCs than hepatocytes (Fig. 1A). Additionally, E6AP was up-regulated in primary HSCs during culture activation with the increase of α-SMA, the HSC transdifferentiation marker (Fig. 1B). Furthermore, we isolated HSCs from the mice treated with vehicle or CCl_4. E6AP was up-regulated in HSCs from CCl_4–injected mice (Fig. 1C). Next, we investigated E6AP expression after TGF-β stimulation with different time and concentrations in LX-2 cells, immortalized human HSC cell lines. E6AP was increased after 1-12 h of TGF-β treatment and was peaked at 3 h (Fig. 1D). Additionally, we observed that E6AP was markedly induced by TGF-β treatment and reached a maximum at 2 ng/ml of TGF-β (Fig. 1E). These results suggest that E6AP is overexpressed in activated HSCs during liver fibrogenesis.

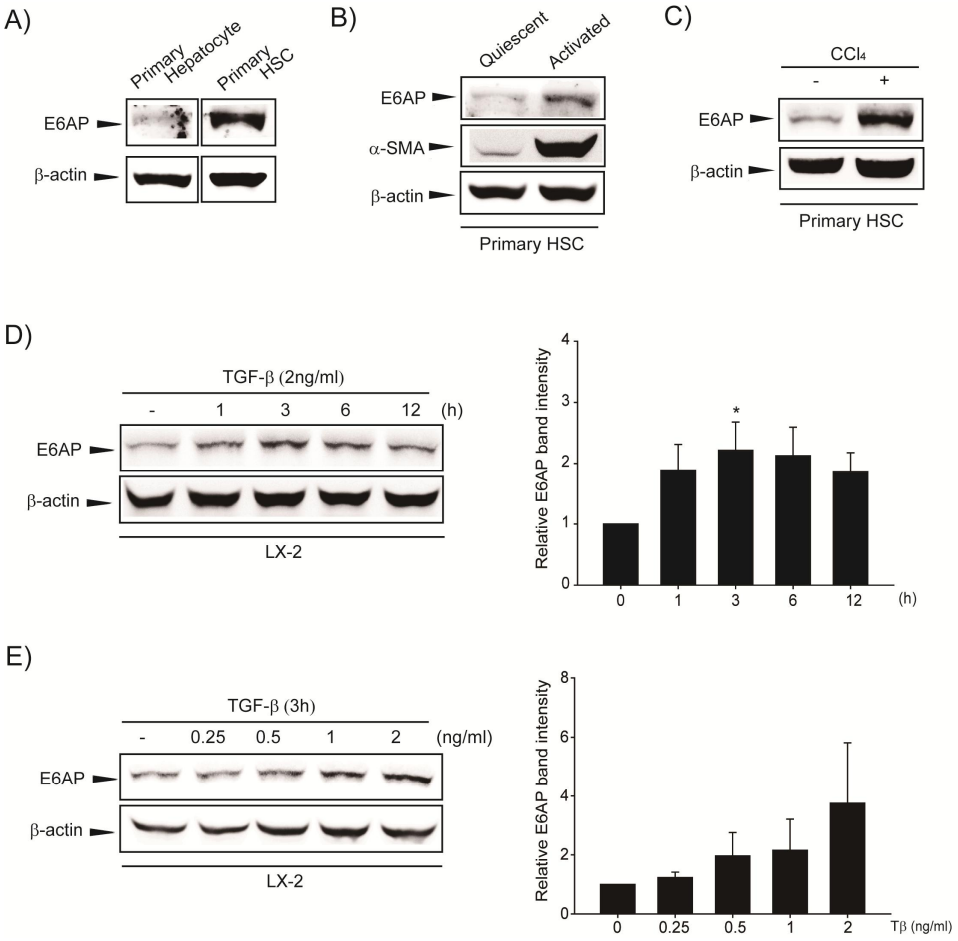

Figure 1. Up-regulation of E6AP during HSCs activation

(A) E6AP expression in primary murine hepatocyte and quiescent hepatic stellate cells (HSCs). (B) E6AP expression in quiescent or activated primary HSCs. Primary HSCs were isolated and cultured in growth medium for 0 (quiescent) or 7 (activated) days, and then the cell lysates (20 μg each) were subjected to immunoblotting. α-smooth muscle actin (α-SMA) was detected as an activation marker of HSC activation and β-actin was used to confirm the equal protein loading. The immunoblot results were confirmed in at least three separate experiments. (c) E6AP expression in primary HSCs from CCl_4-treated mice. Mice were injected with 0.5 mg/kg CCl_4 for 24 h. Primary HSCs were isolated, and E6AP expressions were assessed by immunoblotting. (D) The effect of transforming growth factor-β (TGF-β) treatment on E6AP up-regulation. The time courses of E6AP expression in LX-2 cells treated with TGF-β (2 ng/ml). E6AP levels were assessed by scanning densitometry (n = 3, significant different versus 0 h: *p<0.05). (E) The effect of various concentrations of TGF-β on E6AP induction in LX-2 cells. E6AP protein was immunoblotted in the lysates of cells incubated with 0.25- 2 ng/ml TGF-β for 3 h. E6AP levels were assessed by scanning densitometry (n = 3).

2. The E6AP induction was not derived from either transcriptional regulation or protein stability

To reveal the molecular mechanism governing E6AP overexpression, we investigated E6AP mRNA levels, and discovered that they were not changed in activated HSCs or TGF-β-treated LX-2 cells (Fig. 2A and 2B). Furthermore, we treated a transcription inhibitor, actinomycin-D (ActD) or ActD plus TGF-β to LX-2 cells, and further demonstrated that altered E6AP expression was not due to transcriptional regulation (Fig. 2C). Sequentially, we measured E6AP expression in a protein synthesis inhibitor, cycloheximide (CHX) or CHX plus TGF-β-treated LX-2 cells. E6AP expression was not decreased by CHX and additive TGF-β treatment inferring that the induction of E6AP by TGF-β was not derived from protein stability (Fig. 2D). In additional assays, we found that both a proteasomal inhibitor (MG132, MG) and a lysosomal inhibitor (chloroquine, CQ) did not affect E6AP expression by TGF-β (Fig. 2E and 2F). These results imply that E6AP expression was not controlled by transcriptional regulation or protein stability.

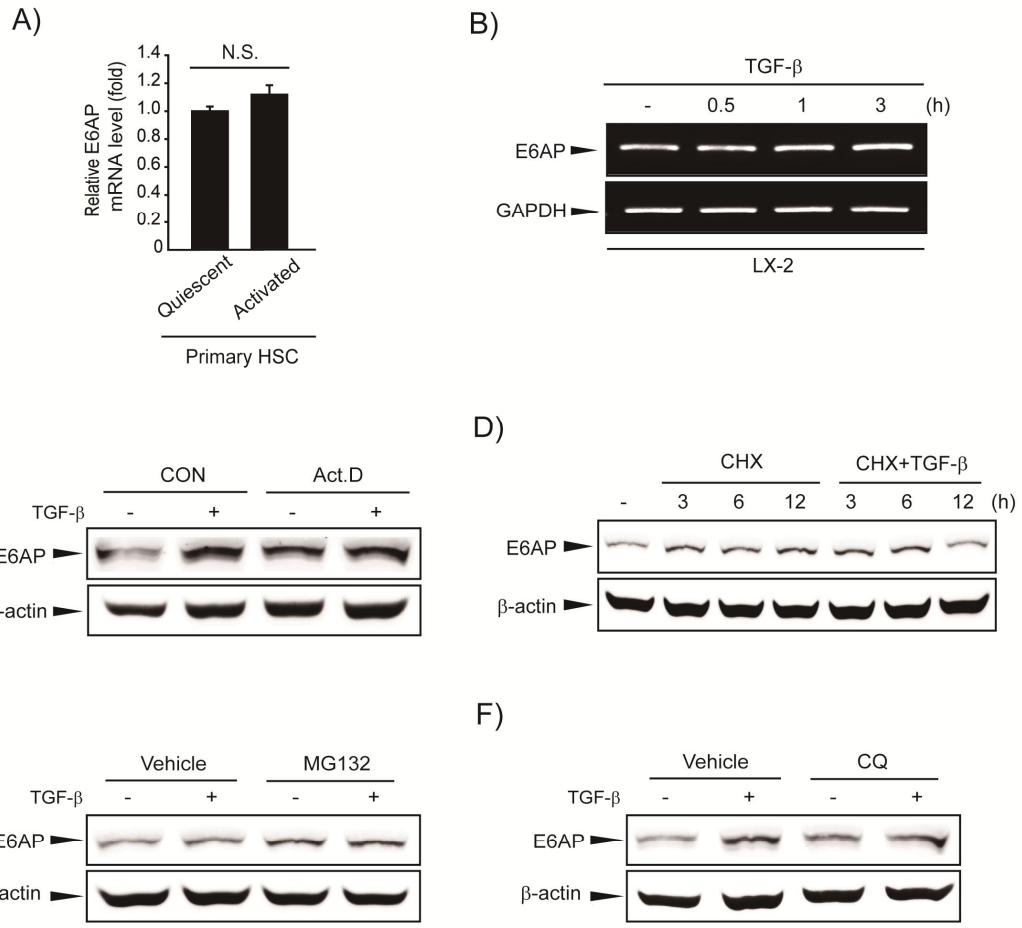

Figure 2. The E6AP induction by neither transcriptional mechanism nor protein stability

(A) Real-time PCR analysis. The E6AP transcript was analyzed, with the mRNA level of GAPDH used as a housekeeping gene in quiescent or activated primary HSCs. The data represents the means±SE of at least three separate experiments. N.S., not significant. (B) RT-PCR analysis. LX-2 cells were treated with 2 ng/ml TGF-β for 0.5- 3 h. Transcriptional levels of E6AP were determined by RT-PCR using GAPDH as an internal control. (C) The effect of actinomycin-D (ActD) on the E6AP induced by TGF-β in LX-2 cells. The cells were treated with 5 μg/mL of ActD in the presence or absence of TGF-β. The level of E6AP protein was monitored after 2 ng/ml TGF-β treatment for 6 h. (D) The effect of cycloheximide (CHX) on E6AP expression. LX-2 cells were incubated with 0.5 μg/mL CHX in the presence or absence of 2 ng/ml TGF-β for the indicated periods. (E) The effect of proteasome inhibition on E6AP induced by TGF-β. LX-2 cells were pretreated with the 10 ng/ml of MG132 for 3 h in the presence or absence of 2 ng/ml TGF-β, and then E6AP expression in the cell lysates was assessed by immunoblotting. (F) The effect of lysosomal inhibition on E6AP induced by TGF-β. LX-2 cells were pretreated with 100 μg/mL of chloroquine (CQ) for 3 h in the presence or absence of 2 ng/ml TGF-β, and then E6AP expression in the cell lysates was assessed by immunoblotting.

3. MicroRNA-302c is identified as a novel regulator of E6AP

MicroRNAs (miRNAs) is a small non-coding RNA molecule (containing about 22 nucleotides) that play important gene regulatory roles via base-pairing with complementary sequences to the mRNAs of protein-coding genes to direct these mRNA silencing. Inhibitory modulation of target leads to decrease in translation efficiency and/or to reduce mRNA level by binding to the 3' UTR of the target mRNA [20, 21]. We searched for putative microRNAs targeting 3′-untranslated region (UTR) of E6AP using the TargetScan 7.1 algorithm (http://www.targetscan.org): miR-219-5p, miR-302-3p/372-3p/373-3p/520-3p, miR-26-5p, miR-218-5p, miR-9-5p, miR-124-3p, miR-141-3p/200a-3p, miR-375 (Fig. 3A). Of the putative miRs, miR-219-5p was predicted as a miRNA with highest affinity to E6AP according to the P_{CT}. The level of miR-219-5p was decreased in TGF-β-treated LX-2 cells as well as primary activated HSCs compared to respective controls. However, we found that miR-219-5p did not affect E6AP expression after miR-219-5p modulation (data not shown). Hence, we focused on miR-302-3p/372-3p/373-3p/520-3p, the miRNAs with second highest probability for matching E6AP. Of these miRNAs candidates, miR-302c was significantly downregulated in primary activated HSCs (Fig. 3B). Moreover, TGF-β treatment to LX-2 cells substantially decreased the level of miR-302c (Fig. 3C). Other members of miR-302 family were not decreased in activated primary HSCs. Additionally, we found that highly conserved and miR-302c recognition sites were present in the 3'-UTR region of E6AP mRNA (Fig. 3D, upper). To demonstrate whether miR-302c directly inhibits E6AP synthesis, E6AP expression was examined after miR-302 modulation using its mimic or inhibitor. E6AP was diminished by miR-302c mimic transfection, conversely increased by miR-302c inhibitor transfection in LX-2 cells (Fig. 3D, lower). We then assessed the functional role of miR-302c in fibrogenesis. miR-302c modulation changed plasminogen activator inhibitor 1 (PAI-1) expression levels.

Additionally, miR-302c inhibitor or mimic transfection appropriated changed luciferase activity from E6AP-3'-UTR in LX-2 cells (Fig. 3E). These results indicated that E6AP overexpression was derived from miR-302c dysregulation in activated HSCs.

A)

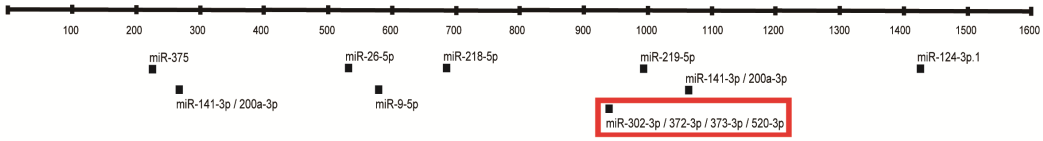

Putative E6AP-targeting miRs

miRNA	P_{CT} (probability of conserved targeting)
miR-219a-5p	0.83
miR-302-3p/372-3p/373-3p/520-3p	0.74
miR-26-5p	0.7
miR-218-5p	0.7
miR-9-5p	0.68
miR-124-3p.1	0.38
miR-141-3p/200a-3p	0.36
miR-375	0.35
TargetScan 7.1 algorithm	

B)

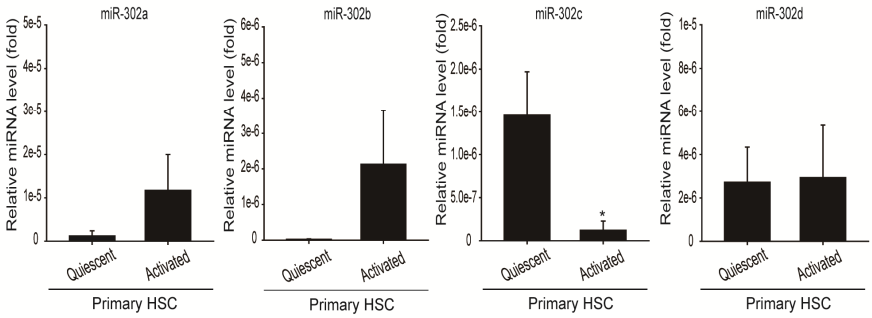

C)

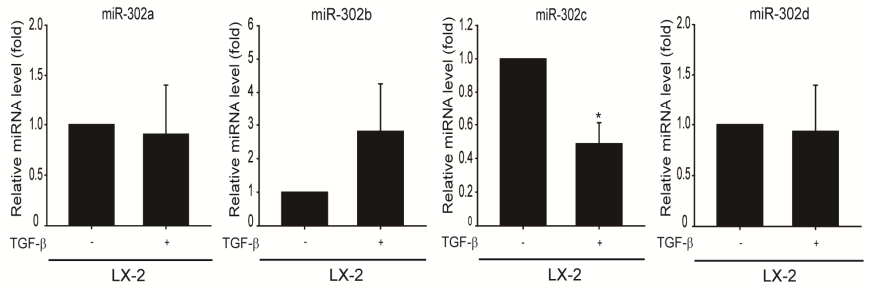

D)

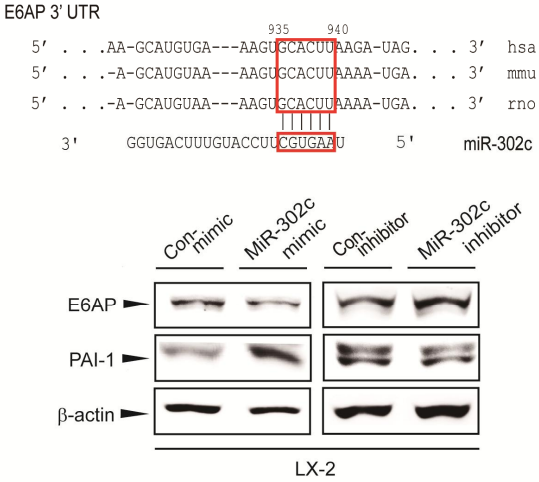

E)

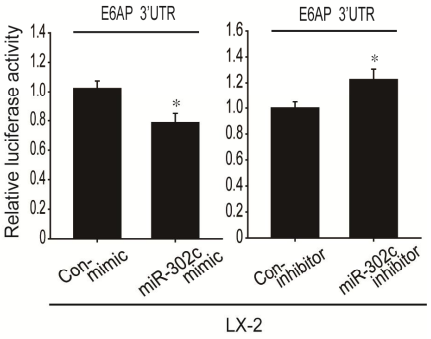

Figure 3. Inhibition of E6AP translation by miR-302c

(A) The locations of the predicted miRNA binding sites within the 3'UTR of E6AP mRNA. (B) Real-time RT-PCR assays for the miR-302a/302b/302c/302d in quiescent or activated primary HSCs. Data were normalized against the levels of U6 small RNA. The data are the means and standard errors of at least three separate experiments (significant as compared with primary quiescent HSCs, $*p<0.05$). (C) Real-time RT-PCR assays for the candidate miRs in LX-2 cells. LX-2 cells were treated with 2 ng/ml TGF-β for 30 min. The data are the means and standard errors of at least three separate experiments (significant as compared with vehicle-treated LX-2 cells, $*p<0.05$). (D) Upper: Alignments of miR-302c binding to the 3'-UTRs of E6AP mRNAs. Lower: Effect of miR-302c on E6AP and fibrogenic gene expression. LX-2 cells were transfected with Con-mimic or miR-302c mimic for 24 h and transfected with Con-inhibitor or miR-302c inhibitor for 24 h. E6AP expression and PAI-1 protein level was detected by immunoblotting with lysates transfected with miR-302c mimic or inhibitor with their respective controls in LX-2 cells. (E) Effect of miR-302c mimic or inhibitor on E6AP 3' UTR reporter assays. Left: Cells were transfected with Con-mimic or miR-302c mimic, and E6AP 3' UTR reporter. Right: Cells were transfected with Con-inhibitor or miR-302c inhibitor, and E6AP 3' UTR reporter. The data are the means and standard errors of at least three separate experiments (significant as compared with Con-transfected controls, $*p<0.05$; significant as compared between miR-302c mimic or inhibitor-transfected cells).

4. The E6AP overexpression inhibits TGF-β-induced hepatic fibrogenesis

Next, we explored the role of E6AP on TGF-β-induced fibrogenic gene expression and related signaling pathway. The treatment of LX-2 cells to TGF-β increased PAI-1 in the MOCK-transfected cells, and this was attenuated by E6AP overexpression (Fig. 4A). Similarly, TGF-β-induced PAI-1 expression was not decreased by E6AP siRNA in LX-2 cells (Fig. 4B). Further assay was performed with a catalytically inactive mutant of E6AP (termed C833A), which cannot form a thiol ester with ubiquitin [22]. Interestingly, C833A exerted no effect on PAI-1 expression against E6AP (Fig. 4C). To determine the possible link between E6AP and TGF-β signaling, we observed luciferase activity from a Smad-binding element (SBE)-driven reporter. E6AP failed to repress SBE luciferase activity by TGF-β treatment (Fig. 4D). Consistently, when we investigated the effect of E6AP on TGF-β-dependent Smad phosphorylation, we could not observe any effect on Smad3 phosphorylation against E6AP (Fig. 4E). Hence, these data imply that E6AP attenuated TGF-β-dependent fibrogenesis via Smad-independent pathway.

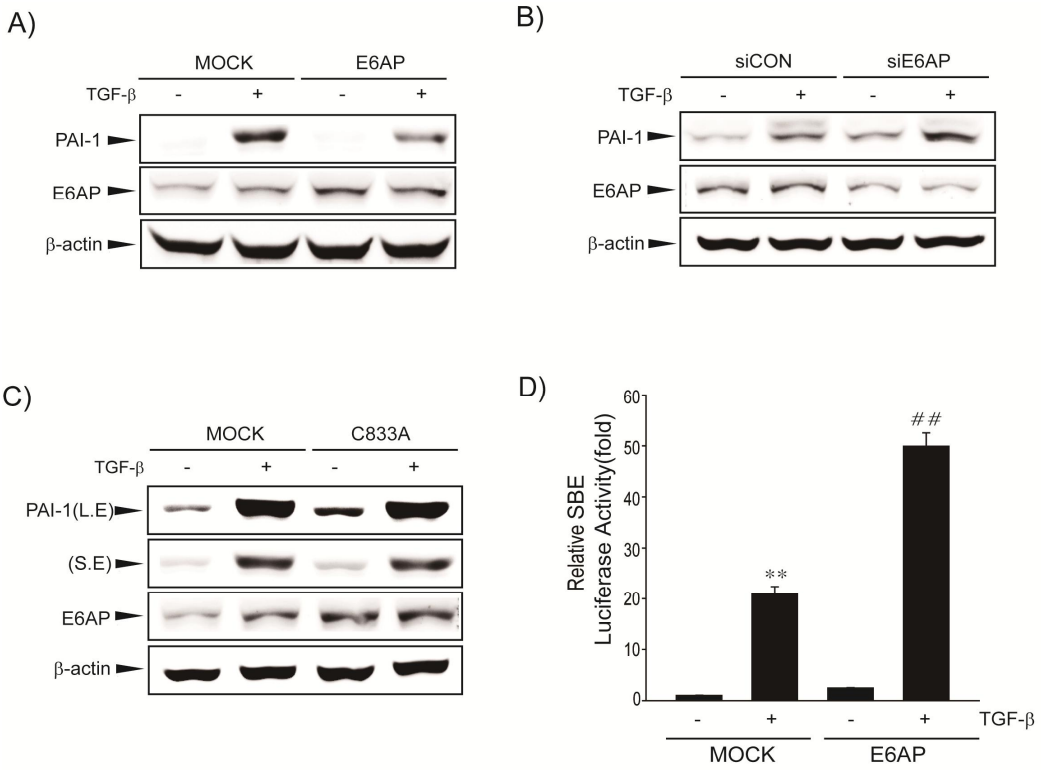

Figure 4. The effect of E6AP on hepatic fibrogenesis in LX-2 cell

(A) Effect of E6AP on TGF-β-induced fibrogenic gene expression. LX-2 cells were transfected with pCMV4 (MOCK) or pCMV4-E6AP (E6AP) for 24 h and then treated with 1 ng/ml TGF-β for 3 h. PAI-1 level was determined by immunoblotting. E6AP expression was confirmed by immunoblotting with lysates from MOCK- or E6AP-transfected cells. (B) Effect of E6AP knockdown on TGF-β-mediated fibrogenic gene expression. LX-2 cells were transfected with control siRNA (siCon) or E6AP siRNA (siE6AP) for 24 h and then treated with 1 ng/ml TGF-β for 3 h. (C) Effect of E6AP mutant (C833A) on TGF-β-induced fibrogenic gene expression. LX-2 cells were transfected with MOCK or C833A for 24 h and then treated with 1 ng/ml TGF-β for 3 h. PAI-1 level was determined by immunoblotting. (D) Effect of E6AP on Smad binding element (SBE) luciferase activity by TGF-β treatment. Cells were transfected with SBE luciferase construct. Transfected cells were treated with 1 ng/ml TGF-β for 3 h. Results represent the means ± SE of three replicates (significant as compared with vehicle-treated controls, **$p<0.01$; significant as compared with TGF-β alone ##$p<0.01$). (E) Effect of TGF-β-mediated Smad3 phosphorylation by E6AP. Cells were transfected as described above and treated with 1 ng/ml TGF-β for 30 min, and the cell lysates were immunoblotted for examination of Smad3 phosphorylation. Results were confirmed by repeated experiments.

5. AP-1 inhibition by E6AP contributes to antifibrogenic effect

To reveal the other signaling pathway to control the antifibrogenic effect of E6AP, we sought to determine the role of mitogen-activated protein kinases (MAPKs) signaling since TGF-β might activate other molecules such as MAPKs [23]. The treatment of MOCK-transfected LX-2 cells with TGF-β-enhanced MAPK phosphorylation including JNK, p38, and ERK. However, E6AP overexpression suppressed the increased MAPK activity by TGF-β (Fig. 5A). Next, we measured AP-1-dependent luciferase activity to assess the inhibitory effect of E6AP on TGF-β -mediated AP-1 activation. We found that increased AP-1 luciferase activity by TGF-β was suppressed by E6AP overexpression. (Fig. 5B). AP-1 is a transcription factor composed of the Jun and Fos or activating transcription factor (ATF) and acts as a heterodimer of Jun and Fos [24]. Interestingly, E6AP overexpression attenuated the effect of TGF-β on phosphorylation of c-Jun and c-Fos (Fig. 5C). Overexpression of c-Jun reversed the antifibrogenic effect of E6AP, corroborative of the connections c-Jun and E6AP (Fig. 5D). Our results demonstrated that E6AP-mediated antifibrogenesis in HSCs might be associated with attenuation of c-Jun-dependent AP-1 activation.

A)

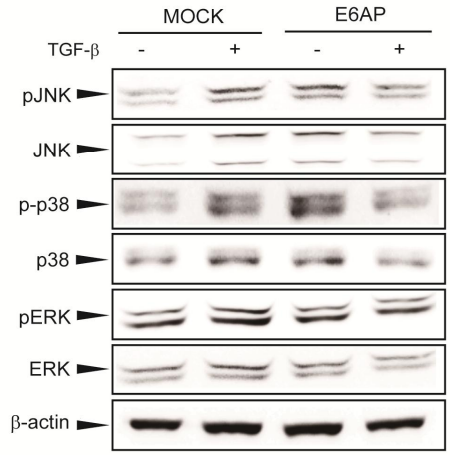

B)

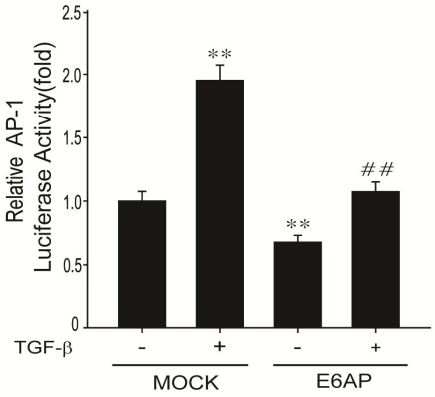

C)

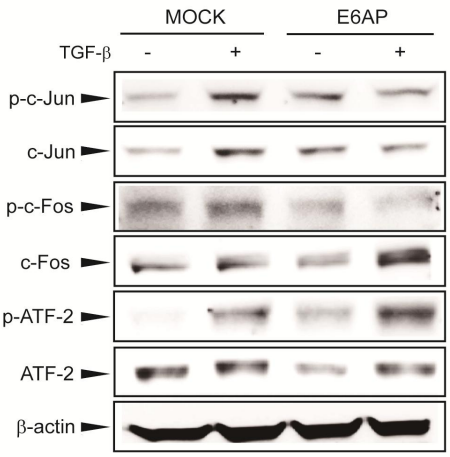

D)

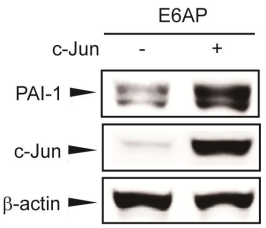

Figure 5. Association of AP-1 with the E6AP effect on hepatic fibrogenesis in LX-2 cell.

(A) Effect of E6AP on TGF-β-induced mitogen-activated protein kinase (MAPK) phosphorylation. LX-2 cells were transfected with MOCK or E6AP for 24 h and then treated with 1 ng/ml TGF-β for 3 min. (B) Effect of E6AP on AP-1 luciferase activity by TGF-β treatment. LX-2 cells were transfected with AP-1 luciferase construct in combination with E6AP (or MOCK) and treated with 1 ng/ml TGF-β for 3 h. Results represent the means ± SE of three replicates (significant as compared with vehicle-treated controls, **$p<0.01$; significant as compared with TGF-β alone ##$p<0.01$). (C) Effect of E6AP on TGF-β-mediated c-Junphosphorylation. Cells were transfected as described above and treated with 2 ng/ml TGF-β for 5 min, and the cell lysates were immunoblotted for examination of c-Jun phosphorylation. Results were confirmed by repeated experiments. (D) The role of c-Jun in E6AP-mediated antifibrogenic effect. LX-2 cells were transfected with E6AP in combination with c-Jun (or MOCK). c-Jun expression was confirmed by immunoblotting with lysates from transfected cells.

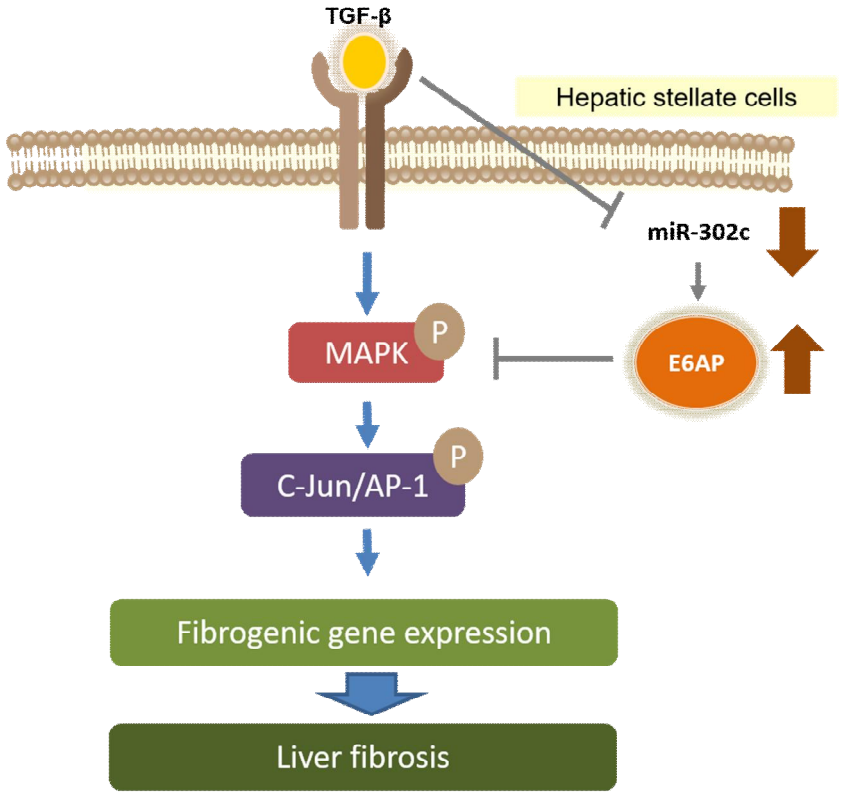

Figure 6. A schematic diagram illustrating the proposed mechanism, by which E6AP induction suppresses TGF-β-mediated fibrogenensis.

IV. DISCUSSION

TGF-β stimulates the synthesis and deposition of various ECM components such as various types of collagen, laminin, and fibronectin during liver fibrosis [25]. E3 ligases can interact with a various substrates and regulate their expression levels which are associated with TGF-β signaling [26]. Although E6AP has been reported that regulates important cellular processes including signal transduction, transcription, cell survival, apoptosis, and DNA repair [27], its expression as well as role on liver fibrosis remain to be revealed. In the current study, we discovered for the first time that E6AP is elevated during HSC activation, suggesting the close relationship between E6AP and liver fibrosis. The data showing that E6AP was up-regulated in HSCs isolated from the CCl_4-treated mice and TGF-β-treated LX-2 cells also strengthened our findings. Our results show that E6AP expression was more abundant in HSCs than in hepatocytes, implying the importance role of E6AP in HSC biology.

MicroRNAs recently emerged as a class of small RNAs that negatively regulate gene expression by binding to the 3'-UTR of their target mRNA. They regulate normal developmental processes, including differentiation and proliferation, as well as hepatic disease development and progression with multiple and diverse targets [28]. In addition, a various aspects of HSC biology are also governed by miRNAs; miR-27a/b regulate HSCs transactivation, miR-15/16 are involved in HSC proliferation, and miR-29 family inhibit a number of fibrosis-related proteins [29-31]. Our study identified that miR-302c as a new regulator of E6AP controls TGF-β-mediated fibrogenesis during HSC activation. We could not observe that E6AP induction was due to either transcriptional or protein stability. These outcomes enable us to investigate the involvement of miRNAs, another major post-

transcriptional mechanism. miR-302c was markedly downregulated during HSC activation and TGF-β treatment in HSCs, and that miR-302c suppressed E6AP expression via binding to 3'-UTR of E6AP mRNA, supports our conclusion that miR-302c dysregulation was a regulatory mechanism of E6AP overexpression in HSCs. The effect of miR-302c on fibrogenic gene indicated that miR-302c dysregulation affected fibrogenensis in HSCs through E6AP regulation. Despite the known effect of miR-302c on self-renewal and pluripotency processes, neural differentiation, and progression of liver cancer [32], the role of miR-302c in the HSC activation has never been studied. Therefore, our finding showing the role of miR-302c in the E6AP expression may provide a key strategy for antifibrotic therapy.

E6AP, which is known as a HECT-type E3 ligase, has a variety substrate proteins; p53 [13], β-catenin [33], ErBb2 [34], peroxiredoxin 1 [35], CCAAT/enhancer binding protein alpha (C/EBPα), and TSC2 [36]. Our result showing that catalytically inactive mutant of E6AP unable to suppress TGF-β-mediated PAI-1 induction, suggests that E6AP ubiquitinated TGF-β signaling-related proteins. As an effect to reveal a direct target of E6AP, several components of TGF-β signaling (Smad 2/3, Smad7, TGF-β receptor I/II) were detected after E6AP overexpression with or without TGF-β treatment. Unfortunately, we could observe that none of the above mentioned proteins were affected by E6AP modulation. Since total MAPK levels changed by TGF-β-treated E6AP overexpression were downregulated, we might assume that E6AP ubiquitinated MAPKs thereby attenuating AP-1 activity under TGF-β stimulation. Further research is needed to identify the substrate of E6AP during HSC activation.

Specific serine/threonine kinase receptors and Smads are well-established effectors in TGF-β signaling, but it is also accepted that additional TGF-β responses control the activation of Smad2/3-independent pathways such as MAPK [37, 38]. In our data, E6AP inhibited TGF-

β-mediated fibrogenesis via activation of MAPK. JNK, p38, and ERK activation induces HSC proliferation and HSC activation in response to TGF-β [39-41]. However, a report has demonstrated that JNK and p38 have distinct and opposed roles in HSCs [42-44]. Despite the reports on the conflicting roles of MAPKs in HSC biology [42-44], our finding showed that JNK, p38, and ERK were involved in antifibrogenic effect of E6AP. Because MAPKs regulate various mechanisms related to liver pathophysiology with common and different biological functions [45-47], further study is necessary to determine discrete roles of MAPKs during HSC activation.

Collectively, our study has revealed that E6AP is overexpressed during transdifferentiation of HSCs mediated by miR-302c dysregulation, and this event suppresses MAPK phosphorylation and subsequent c-Jun-dependent AP-1 activation. These findings provide new insight into the regulation of a key signaling pathway which attenuates hepatic fibrogenesis consequent liver fibrosis.

V. REFERENCES

1. Seki, E. and D.A. Brenner, Recent advancement of molecular mechanisms of liver fibrosis. J Hepatobiliary Pancreat Sci, 2015. **22**(7): p. 512-8.
2. Huang, Y., X. Deng, and J. Liang, Modulation of hepatic stellate cells and reversibility of hepatic fibrosis. Exp Cell Res, 2017. **352**(2): p. 420-426.
3. Friedman, S.L., Hepatic stellate cells: protean, multifunctional, and enigmatic cells of the liver. Physiol Rev, 2008. **88**(1): p. 125-72.
4. Tacke, F. and R. Weiskirchen, Update on hepatic stellate cells: pathogenic role in liver fibrosis and novel isolation techniques. Expert Rev Gastroenterol Hepatol, 2012. **6**(1): p. 67-80.
5. Guo, W., et al., Ubiquitin-proteasome pathway function is required for lens cell proliferation and differentiation. Invest Ophthalmol Vis Sci, 2006. **47**(6): p. 2569-75.
6. Lecker, S.H., A.L. Goldberg, and W.E. Mitch, Protein degradation by the ubiquitin-proteasome pathway in normal and disease states. J Am Soc Nephrol, 2006. **17**(7): p. 1807-19.
7. Cai, Y., et al., Smurf2, an E3 ubiquitin ligase, interacts with PDE4B and attenuates liver fibrosis through miR-132 mediated CTGF inhibition. Biochim Biophys Acta, 2017.
8. Hasegawa, D., et al., E3 ubiquitin ligase synoviolin is involved in liver fibrogenesis. PLoS One, 2010. **5**(10): p. e13590.
9. Ebisawa, T., et al., Smurf1 interacts with transforming growth factor-beta type I receptor through Smad7 and induces receptor degradation. J Biol Chem, 2001. **276**(16): p. 12477-80.
10. Fukasawa, H., et al., Down-regulation of Smad7 expression by ubiquitin-dependent

degradation contributes to renal fibrosis in obstructive nephropathy in mice. Proc Natl Acad Sci U S A, 2004. **101**(23): p. 8687-92.

11. Tan, R., et al., Smad ubiquitination regulatory factor-2 in the fibrotic kidney: regulation, target specificity, and functional implication. Am J Physiol Renal Physiol, 2008. **294**(5): p. F1076-83.
12. Murakami, G., et al., Cooperative inhibition of bone morphogenetic protein signaling by Smurf1 and inhibitory Smads. Mol Biol Cell, 2003. **14**(7): p. 2809-17.
13. Hengstermann, A., et al., Complete switch from Mdm2 to human papillomavirus E6-mediated degradation of p53 in cervical cancer cells. Proc Natl Acad Sci U S A, 2001. **98**(3): p. 1218-23.
14. Matentzoglu, K. and M. Scheffner, Ubiquitin ligase E6-AP and its role in human disease. Biochem Soc Trans, 2008. **36**(Pt 5): p. 797-801.
15. Raghu, D., et al., E6AP promotes prostate cancer by reducing p27 expression. Oncotarget, 2017. **8**(26): p. 42939-42948.
16. Levav-Cohen, Y., et al., E6AP is required for replicative and oncogene-induced senescence in mouse embryo fibroblasts. Oncogene, 2012. **31**(17): p. 2199-209.
17. Wolyniec, K., et al., The E6AP E3 ubiquitin ligase regulates the cellular response to oxidative stress. Oncogene, 2013. **32**(30): p. 3510-9.
18. Munakata, T., et al., Hepatitis C virus induces E6AP-dependent degradation of the retinoblastoma protein. PLoS Pathog, 2007. **3**(9): p. 1335-47.
19. Koo, J.H., et al., Endoplasmic Reticulum Stress in Hepatic Stellate Cells Promotes Liver Fibrosis via PERK-Mediated Degradation of HNRNPA1 and Up-regulation of SMAD2. Gastroenterology, 2016. **150**(1): p. 181-193 e8.
20. Bartel, D.P., MicroRNAs: genomics, biogenesis, mechanism, and function. Cell, 2004.

116(2): p. 281-97.

21. Guo, H., et al., Mammalian microRNAs predominantly act to decrease target mRNA levels. Nature, 2010. **466**(7308): p. 835-40.
22. Tomaic, V. and L. Banks, Angelman syndrome-associated ubiquitin ligase UBE3A/E6AP mutants interfere with the proteolytic activity of the proteasome. Cell Death Dis, 2015. **6**: p. e1625.
23. Gui, T., et al., The Roles of Mitogen-Activated Protein Kinase Pathways in TGF-beta-Induced Epithelial-Mesenchymal Transition. J Signal Transduct, 2012. **2012**: p. 289243.
24. Gangnuss, S., et al., Regulation of MAPK activation, AP-1 transcription factor expression and keratinocyte differentiation in wounded fetal skin. J Invest Dermatol, 2004. **122**(3): p. 791-804.
25. Casini, A., et al., Regulation of extracellular matrix synthesis by transforming growth factor beta 1 in human fat-storing cells. Gastroenterology, 1993. **105**(1): p. 245-53.
26. Izzi, L. and L. Attisano, Regulation of the TGFbeta signalling pathway by ubiquitin-mediated degradation. Oncogene, 2004. **23**(11): p. 2071-8.
27. Kim, Y., et al., E6AP gene suppression and characterization with in vitro selected hammerhead ribozymes. Cancer Gene Ther, 2003. **10**(9): p. 707-16.
28. Lakner, A.M., H.L. Bonkovsky, and L.W. Schrum, microRNAs: fad or future of liver disease. World journal of gastroenterology : WJG, 2011. **17**(20): p. 2536-42.
29. Ji, J., et al., Over-expressed microRNA-27a and 27b influence fat accumulation and cell proliferation during rat hepatic stellate cell activation. FEBS Lett, 2009. **583**(4): p. 759-66.
30. Guo, C.J., et al., miR-15b and miR-16 are implicated in activation of the rat hepatic stellate cell: An essential role for apoptosis. J Hepatol, 2009. **50**(4): p. 766-78.

31. Li, J., et al., Roles of microRNA-29a in the antifibrotic effect of farnesoid X receptor in hepatic stellate cells. Mol Pharmacol, 2011. **80**(1): p. 191-200.

32. Wang, Z.M., et al., MicroRNAs are involved in the self-renewal and differentiation of cancer stem cells. Acta Pharmacol Sin, 2013. **34**(11): p. 1374-80.

33. Birch, S.E., et al., Expression of E6AP and PML predicts for prostate cancer progression and cancer-specific death. Ann Oncol, 2014. **25**(12): p. 2392-7.

34. Narisawa-Saito, M., et al., HPV16 E6-mediated stabilization of ErbB2 in neoplastic transformation of human cervical keratinocytes. Oncogene, 2007. **26**(21): p. 2988-96.

35. Nasu, J., et al., E6AP ubiquitin ligase mediates ubiquitin-dependent degradation of peroxiredoxin 1. J Cell Biochem, 2010. **111**(3): p. 676-85.

36. Zheng, L., et al., E3 ubiquitin ligase E6AP-mediated TSC2 turnover in the presence and absence of HPV16 E6. Genes Cells, 2008. **13**(3): p. 285-94.

37. Massague, J. and Y.G. Chen, Controlling TGF-beta signaling. Genes Dev, 2000. **14**(6): p. 627-44.

38. Derynck, R. and Y.E. Zhang, Smad-dependent and Smad-independent pathways in TGF-beta family signalling. Nature, 2003. **425**(6958): p. 577-84.

39. Kostadinova, R., et al., GW501516-activated PPARbeta/delta promotes liver fibrosis via p38-JNK MAPK-induced hepatic stellate cell proliferation. Cell Biosci, 2012. **2**(1): p. 34.

40. Varela-Rey, M., et al., p38 MAPK mediates the regulation of alpha1(I) procollagen mRNA levels by TNF-alpha and TGF-beta in a cell line of rat hepatic stellate cells(1). FEBS Lett, 2002. **528**(1-3): p. 133-8.

41. Khimji, A.K., R. Shao, and D.C. Rockey, Divergent transforming growth factor-beta signaling in hepatic stellate cells after liver injury: functional effects on ECE-1 regulation. Am J Pathol, 2008. **173**(3): p. 716-27.

42. Schnabl, B., et al., TAK1/JNK and p38 have opposite effects on rat hepatic stellate cells. Hepatology, 2001. **34**(5): p. 953-63.

43. Hong, I.H., et al., JNK1 and JNK2 regulate alpha-SMA in hepatic stellate cells during CCl4 -induced fibrosis in the rat liver. Pathol Int, 2013. **63**(10): p. 483-91.

44. Kluwe, J., et al., Modulation of hepatic fibrosis by c-Jun-N-terminal kinase inhibition. Gastroenterology, 2010. **138**(1): p. 347-59.

45. Hirosumi, J., et al., A central role for JNK in obesity and insulin resistance. Nature, 2002. **420**(6913): p. 333-6.

46. Chen, N., et al., Differential gene expression profiles of Jnk1- and Jnk2-deficient murine fibroblast cells. Cancer Res, 2002. **62**(5): p. 1300-4.

47. Wang, Y., et al., Tumor necrosis factor-induced toxic liver injury results from JNK2-dependent activation of caspase-8 and the mitochondrial death pathway. J Biol Chem, 2006. **281**(22): p. 15258-67.